

THE DESIGN AND EVALUATION
OF A
MICROWAVE PHASE MEASUREMENT SYSTEM

William Alan Weis

United States Naval Postgraduate School



THESIS

THE DESIGN AND EVALUATION
OF A
MICROWAVE PHASE MEASUREMENT SYSTEM

by

William Alan Weis

Thesis Advisor:

G. E. Schacher

June 1971

Approved for public release; distribution unlimited.

T139920

LIBRARY
NAVAL POSTGRADUATE SCHOOL
MONTEREY, CALIF. 93940

The Design and Evaluation
of a
Microwave Phase Measurement System

by

William Alan Weis
Major, United States Army
B.S., United States Military Academy, 1961

Submitted in partial fulfillment of the
requirements for the degree of

MASTER OF SCIENCE IN PHYSICS

from the

NAVAL POSTGRADUATE SCHOOL
June 1971

Thesis
SW 375
C-1

ABSTRACT

This thesis was undertaken to ascertain the feasibility of producing an accurate phase measurement system using standard components normally available in the laboratory or those that could be purchased relatively inexpensively. Several systems are discussed and two of them were physically evaluated. It was concluded that it was not feasible to build an accurate system without large additional expense; however, if such expense is justifiable, recommendations are given for the construction of an improved system.

TABLE OF CONTENTS

I.	INTRODUCTION -----	4
II.	PHASE MEASUREMENT THEORY -----	6
III.	TRANSMISSION LINE THEORY -----	14
IV.	EQUIPMENT -----	19
V.	EXPERIMENTAL PROCEDURES AND CALIBRATION -----	25
	A. PROCEDURES -----	25
	B. CALIBRATION -----	26
VI.	RESULTS -----	31
VII.	CONCLUSIONS -----	37
	LIST OF REFERENCES -----	39
	INITIAL DISTRIBUTION LIST -----	40
	FORM DD 1473 -----	41

I. INTRODUCTION

To adapt materials to electronic devices, it is often necessary to know their magnetic permeability and/or dielectric constant. These quantities are a measure of the response of a material to magnetic and electric fields, respectively, and both the magnitude and phase of the response are important. One method commonly employed to evaluate the susceptibilities is to measure the amplitude and phase of an electromagnetic wave reflected from the sample.

At microwave frequencies, the measurement of amplitude, or power, is straight forward but measurements of phase are quite time consuming and difficult. Although complete phase bridge systems are available commercially, they are very expensive. Therefore, this thesis was undertaken to ascertain the feasibility of producing an accurate phase measurement system using standard components normally available in the laboratory or those that could be purchased relatively inexpensively. The aim is to build a system that can continuously monitor the phase of the reflected signal over a wide frequency band.

Discussions of phase measurements and transmission line theory are presented in sections II and III, respectively. These discussions are necessarily quite brief and are presented as a reference for the remainder of the paper. Much more extensive treatment of these theories is available in the references listed in the bibliography or in most advanced Electricity and Magnetism books. Section IV contains a discussion of the equipment used during the course of

this work and the experimental procedures and calibration methods are discussed extensively in section V. Finally, the results and conclusions are presented in sections VI and VII.

II. PHASE MEASUREMENT THEORY

In working with microwave systems, the easiest way to measure the phase of a reflected signal is to compare it with a reference signal. The simplest reference signal to use is the wave incident on the sample. Several methods are available for phase detection; however, only two basic systems are covered in the discussion that follows. They are the slotted-line technique for detection of standing waves created by the interference between incident and reflected waves and a phase-bridge system.

For the phase detection systems discussed, the microwave signal was generated by a reflex Klystron and transmitted by X-band rectangular waveguide operating in the TE_{10} mode. The system components will be discussed in detail in section IV.

When a slotted line is placed in a waveguide, it can be used to detect maxima and minima in the standing-wave pattern, thus indicating the phase of the reference signal. It, along with a standing-wave indicator, can also determine voltage standing-wave ratio (VSWR), the ratio of the maximum voltage to the minimum voltage in the standing-wave pattern, giving the amplitude of the reflected signal. By using a short to establish a reference phase and measuring the relative shift of the voltage minimum for a load, a phase angle can be determined. Since the distance between two successive minima or maxima is $\lambda/2$, the phase shift is

$$\theta = \frac{180^\circ \left(\frac{\Delta d}{\lambda/2} \right)}{\lambda/2}$$



where θ is the angular shift and $\frac{1}{\lambda} \Delta d$ is the shift in centimeters of the maxima or minima from a known reference, and λ is the wavelength. This method, as previously discussed, was found to be quite cumbersome and slow.

The phase-bridge method was chosen as the only feasible possibility for a continuous, rapid-phase measuring device and is the subject of this thesis. In the bridge, the incident and reflected signals are combined in a mixer; the output of the mixer is then proportional to the magnitude of both the incident and reflected signals and their relative phase. Several methods are available for this type of phase measurement; however, only three will be described here, two of which are described in much more detail in section IV.

If the incident and reflected signals are added in a mixer and a square-law crystal is used to detect the resultant signal, this resultant signal provides a basis for the determination of the phase angle between the incident and reflected signals. Dyson [Ref. 3] discusses microwave phase measurement in detail in his article. Two modified versions of his systems were selected for experiment by this author. If a hybrid tee, with the E port terminated, is used to add the signals and square-law crystals are used, the voltage output from this crystal will be related to the incident and reflected fields and the angle between them as follows:

$$V \propto E_I^2 + E_R^2 + 2E_I E_R \cos(\phi - \theta), \quad \text{II-1}$$

where E_I and E_R (let $I = E_I$ and $R = E_R$) are the incident and reflected fields, respectively, and ϕ and θ are the phases of these fields

relative to some reference phase. This proportionality is nothing more than the law of cosines and can be seen on the vector diagram (fig. II-1). Since the incident wave is to be used as a reference, θ can be defined as zero.

If a second mixer is placed in the system and preceded by a 90-degree phase shift of the reflected signal before mixing the incident and reflected signals, the voltage detected by a crystal in this mixer will be related to the sine of the angle between the incident and reflected wave as follows:

$$V \propto I^2 + R^2 + 2IR \sin(\phi - \theta). \quad \text{II-2}$$

This equation can be seen more clearly by means of a vector diagram (fig. II-2).

By employing both types of mixing described above simultaneously (with and without 90-degree phase shift), it would be possible to obtain an X-Y plot of the components of the reflected signal. We will refer to the configuration using one mixer as the single-arm system and the one containing two mixers as the double-arm system.

Further advantages can be gained through the use of balanced mixers. When the incident and reflected waves are incident on the collinear arms of a hybrid tee, the outputs of the H and E arms of the hybrid tee will be the sum and difference of the two inputs, respectively. If these two outputs are then combined (added) in a balanced mixer or differential amplifier, the resultant voltage [Ref. 3] is

$$V \propto 4IR \cos(\phi - \theta) \quad \text{II-3}$$

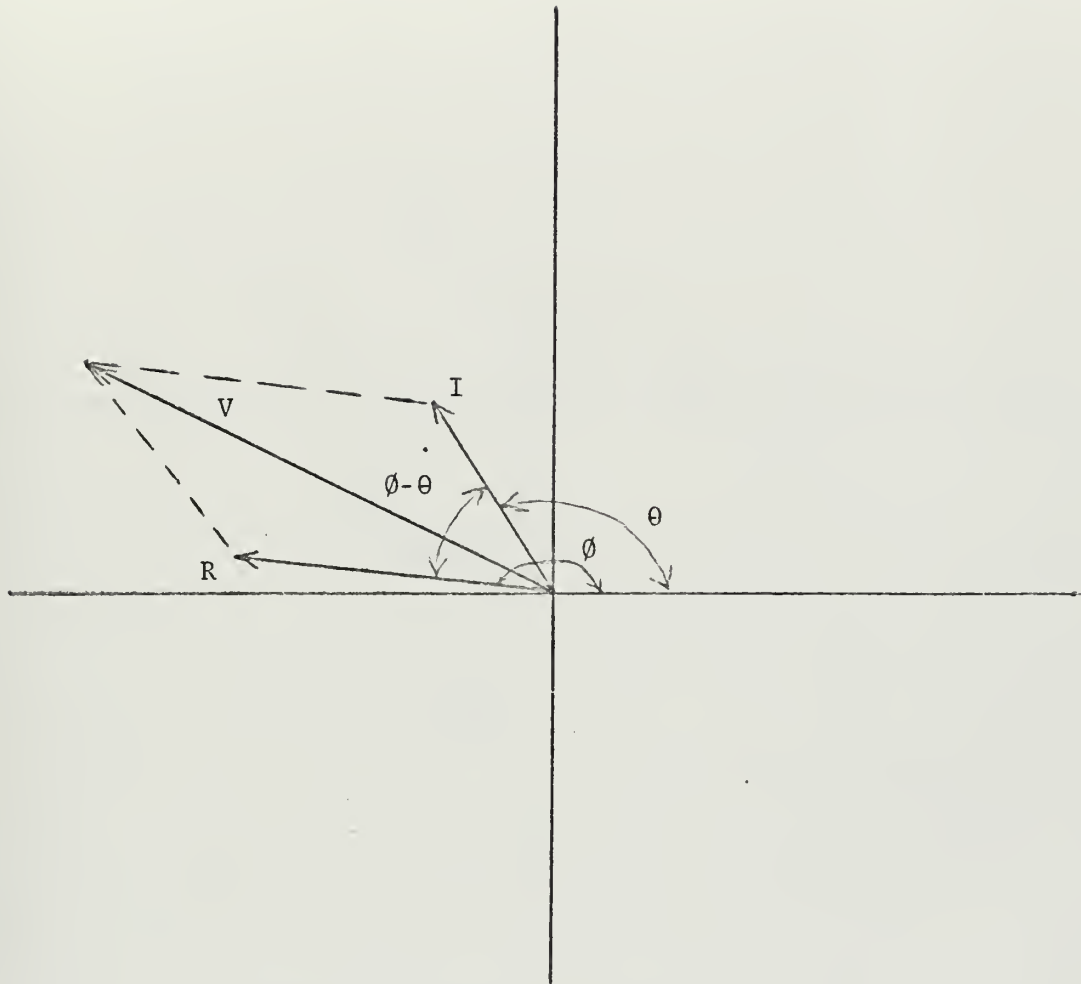


Figure II-1 Vector Diagram of

$$V^2 = I^2 + R^2 + 2IR \cos \phi$$

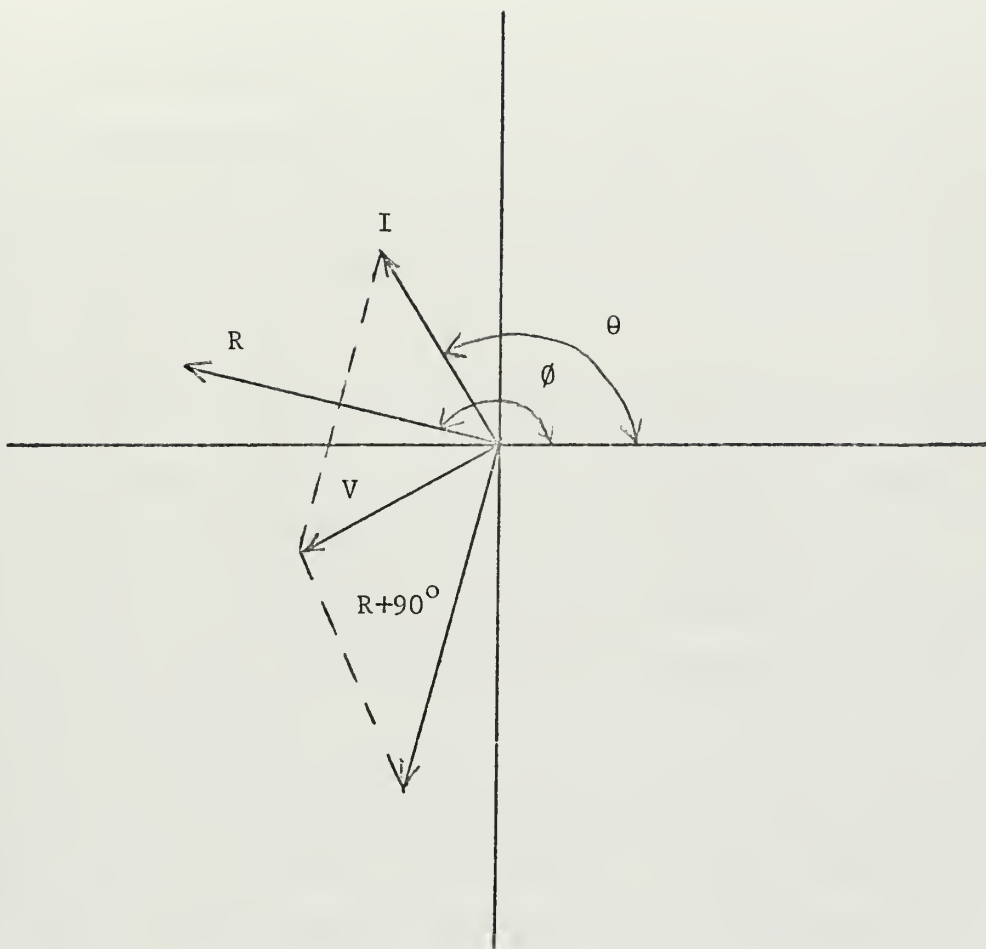


Figure II-2 Vector Diagram of

$$V = I^2 + R^2 - 2IR \sin \phi$$

In this case, the squared terms of the previous equations have cancelled since they are added out of phase in the balanced mixer and the output voltage is directly proportional to the magnitudes of the incident and reflected voltages and the cosine of the angle between them. The use of balanced mixers simplifies the calculations; however, construction of such a system requires extremely well-matched crystal detectors for the two detection arms of the tee, which were not available.

If the voltage detected by a crystal is to be used directly for the calculation of phase angle, the crystal must be a square-law crystal, otherwise extensive calibration will be necessary. When the crystal is square-law, the voltage measured is proportional to E^2 and one arrives at the equations (II-1 through II-3) to be used in the calculations.

A square-law crystal detector is one in which the output voltage is proportional to RF power at the crystal. A typical crystal detector has a current-voltage characteristic which can be approximated by a Taylor Series:

$$i = a_0 + a_1 V + a_2 V^2 + a_3 V^3 + \dots \quad \text{II-4}$$

If the operating point is the origin ($i = 0$ and $v = 0$) then $a_0 = 0$.

If $v = A \cos \omega t$ where A is the amplitude and ω the angular frequency, then

$$i = a_1 A \cos \omega t + a_2 (A \cos \omega t)^2 + a_3 (A \cos \omega t)^3 + \dots \quad \text{II-5}$$

For small signals, all of the terms except the first are negligible and $i = a_1 A \cos \omega t$, a linear relationship between i and v . For larger signals:

$$\begin{aligned}
 i &= a_1 A \cos \omega t + a_2 (A \cos \omega t)^2 \\
 &= a_1 A \cos \omega t + a_2 \frac{A^2}{2} (1 + \cos 2\omega t)
 \end{aligned}
 \tag{II-6}$$

In this case, the current is proportional to the square of the amplitude. For still higher signals, more terms must be included in the expansion and the crystal deviates from its square-law characteristics. The determination of each crystal's square-law range was very critical to the phase measurements described here and will be covered in detail in section V.

Equations II-1 and II-2 can be rearranged in order to give an expression for the phase angle, \emptyset , the desired quantity. After corrections have been applied for power splittings in the system, due to the fact that hybrid tees and 3 db couplers cause the power to be reduced by one-half, \emptyset can be expressed for a single-arm phase bridge as follows:

$$\emptyset = \arccos \left[\frac{V}{I\sqrt{r}} - \frac{1+r}{2\sqrt{r}} \right],
 \tag{II-7}$$

and for a double-arm phase bridge as follows:

$$\emptyset = \arccos \left[\frac{4V_1}{I\sqrt{r}} - \frac{1+r}{2\sqrt{r}} \right],
 \tag{II-8A}$$

$$\emptyset = \arcsin \left[\frac{1+r}{2\sqrt{r}} - \frac{4V_2}{I\sqrt{r}} \right]
 \tag{II-8B}$$

where $r \equiv R/I$, and V_1 and V_2 are the voltages at the in phase and out of phase crystals.

In principle r may be eliminated from equations II-8 to express the phase angle \emptyset as a function of V_1 and V_2 , the measured voltages

at the two mixers. However, equation II-7 cannot be solved for \emptyset and, therefore, the reflection coefficient, r , must be measured separately.

III. TRANSMISSION LINE THEORY

The purpose of this section is to describe the relationship between an impedance measured at one point in a transmission line with a load placed at some other point in the transmission line. A knowledge of transmission line theory allows one to understand and apply this relationship.

The impedance of a microwave circuit is not a clearly defined quantity [Ref. 1] as it is in a simple electrical circuit since it depends on how the other parameters, such as voltage and current, are defined. It can, however, be defined in general as a constant of proportionality between some voltage and current. In many transmission line theory problems, neither the exact definition nor its numerical value is relevant to the determination of the other parameters of the circuit. This is the case in the determination of phase angle in a microwave system where one wishes to observe the effects of a load placed at some point in a uniform transmission line.

In order to understand the method used to establish the relationship between the impedance at one point in the line with a load placed at some other point in the line, the general nature of the circuit parameters needs to be understood.

If V_1 and I_1 represent the voltage and current of an incident wave propagating in the x direction and V_2 and I_2 represent a reflected wave propagating in the x direction, the two travelling waves can be represented as follows:

$$\begin{array}{lll}
\text{incident} & V_1 e^{j(\omega t - \beta x)} & , \quad I_1 e^{j(\omega t - \beta x)}, \\
\text{reflected} & V_2 e^{j(\omega t + \beta x)} & , \quad I_2 e^{j(\omega t + \beta x)},
\end{array}$$

where β , the propagation constant, is equal to 2π divided by the guide wavelength. In terms of a characteristic impedance, Z_o , these can also be written as:

$$\begin{array}{lll}
\text{incident} & V_1 e^{j(\omega t - \beta x)} & , \quad V_1/Z_o e^{j(\omega t - \beta x)}, \\
\text{reflected} & V_2 e^{j(\omega t + \beta x)} & , \quad -V_2/Z_o e^{j(\omega t + \beta)},
\end{array}$$

If we let the impedance, Z , at some point in the line equal the ratio of total voltage to the total current, then:

$$Z = Z_o \frac{1 + V_2/V_1 e^{j2\beta x}}{1 - V_2/V_1 e^{j2\beta x}}$$

If the transmission line is terminated by an impedance Z_L at $x = \ell$, we can express the impedance of the line at x as:¹

$$Z = Z_o \frac{Z_L + jZ_o \tan \beta(\ell - x)}{Z_o + jZ_L \tan \beta(\ell - x)} \quad \text{III-1}$$

The quantities actually measured are the voltages at the incident, reflected, and phase points. From the voltages measured at the incident and reflected ports, we obtain a value for r , the reflection coefficient. The complex reflection coefficient is given by the ratio:²

$$r = V_2/V_1 = \frac{Z_L - Z_o}{Z_L + Z_o} e^{-j2\beta \ell} = \left| \frac{Z_L - Z_o}{Z_L + Z_o} \right| \angle -2\beta \ell + \phi \quad \text{III-2}$$

¹Ginzton, E. L., Microwave Measurements, p. 222, McGraw-Hill, 1957.

²Ibid., p. 223.

where \emptyset is the angle of the vector quantity in the absolute brackets. The absolute value of r depends only on the ratio Z_L/Z_o , but its phase depends both upon the nature of the load and the distance from the load.

Because the equations developed above are quite complicated, they are more easily solved by graphical means. The Smith chart, which is a graphical representation of equation II-2, was the method used for this thesis. The advantage of this chart is that, regardless of the value of Z_L , all possible values of Z_L lie either within the circle $|r| = 1$ or on its periphery.

In order to use the Smith chart for calculations, it is necessary to establish a reference phase from which the circuit parameters can be measured. The reference in this case was a copper short placed in the transmission line where the loads to be tested were subsequently placed. This short was assumed to be purely resistive and to have a reflection coefficient of one.

The nature of a load is completely determined from its geometry. Loads can be purely resistive, purely capacitive, purely inductive, or combinations of these. When a load, or conducting obstacle, is placed in a transmission line, its geometry determines whether the imaginary part of the impedance is inductive susceptance, or capacitive susceptance. Susceptance, rather than reactance, was used for calculations because the expressions for conducting obstacles are more commonly given in susceptance.

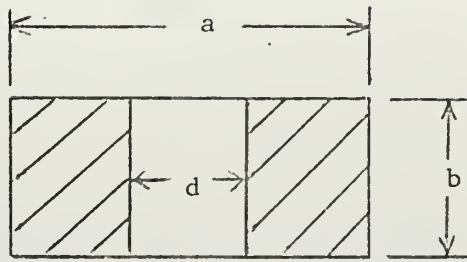
Figure III-1 shows the construction of the loads, or irises as they are normally called. The relative susceptance of a symmetric inductive iris can be expressed [Ref. 4] as:

$$B/Y_o = -\lambda_g/a \cot^2 \frac{\pi d}{2a} \quad \text{III-3}$$

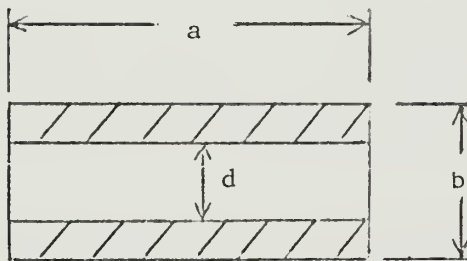
and the relative susceptance of a symmetric capacitive iris can be expressed as:

$$B/Y_o = 4b/\lambda_g \ln \csc \pi d/2b \quad \text{III-4}$$

where a , b , and d are the dimensions indicated in fig. III-1, Y_o is the characteristic admittance of the waveguide, which cancels out in the calculations, and λ_g is the guide wavelength. Since the susceptance of the irises can be very easily calculated, a check on the accuracy of the phase-measurement system is readily available. One needs only to measure the phase of the signal reflected from an iris and compare it to the phase calculated using equations III-3 and III-4.



a. Inductive Iris



b. Capacitive Iris

Figure III-1

IV. EQUIPMENT

All measurements were made at a frequency of 9.172 Ghz in X-band rectangular waveguide.

The single arm system is shown in figure IV-1. Power for the system was provided by a Hewlett Packard 715A Klystron power supply and the RF signal was generated by an X-13 Reflex Klystron. The Klystron is followed by an isolator then a Hewlett Packard X382A Precision Variable Attenuator (referred to as AT-1). This attenuator, with a range of 0-50 db, had two basic purposes: one, to control the power level to the whole system; the second to insure that the crystal detector at which phase was measured was kept within its square-law range.

A 10 db coupler now provides the incident signal input to the phase bridge portion of the system (this portion of the system is indicated by dotted lines). The straight portion of the waveguide next contains a Uniline Isolator to maintain the separation of the incident and reflection arms of the circuit, then a reversed 10 db coupler which provides the reflected signal to the phase bridge portion of the system. Next is the slotted line, then the load. The slotted line consists of a Hewlett Packard Model 809B Universal Probe, X810B Slotted Line Carriage, and a Hewlett Packard Model 444A Untuned Probe and Crystal Detector. The slotted line was used mainly in the preliminary experimental stages to verify the waveguide wavelength, check voltage standing-wave ratios, and to check the shift of maxima and minima due to a movable short.

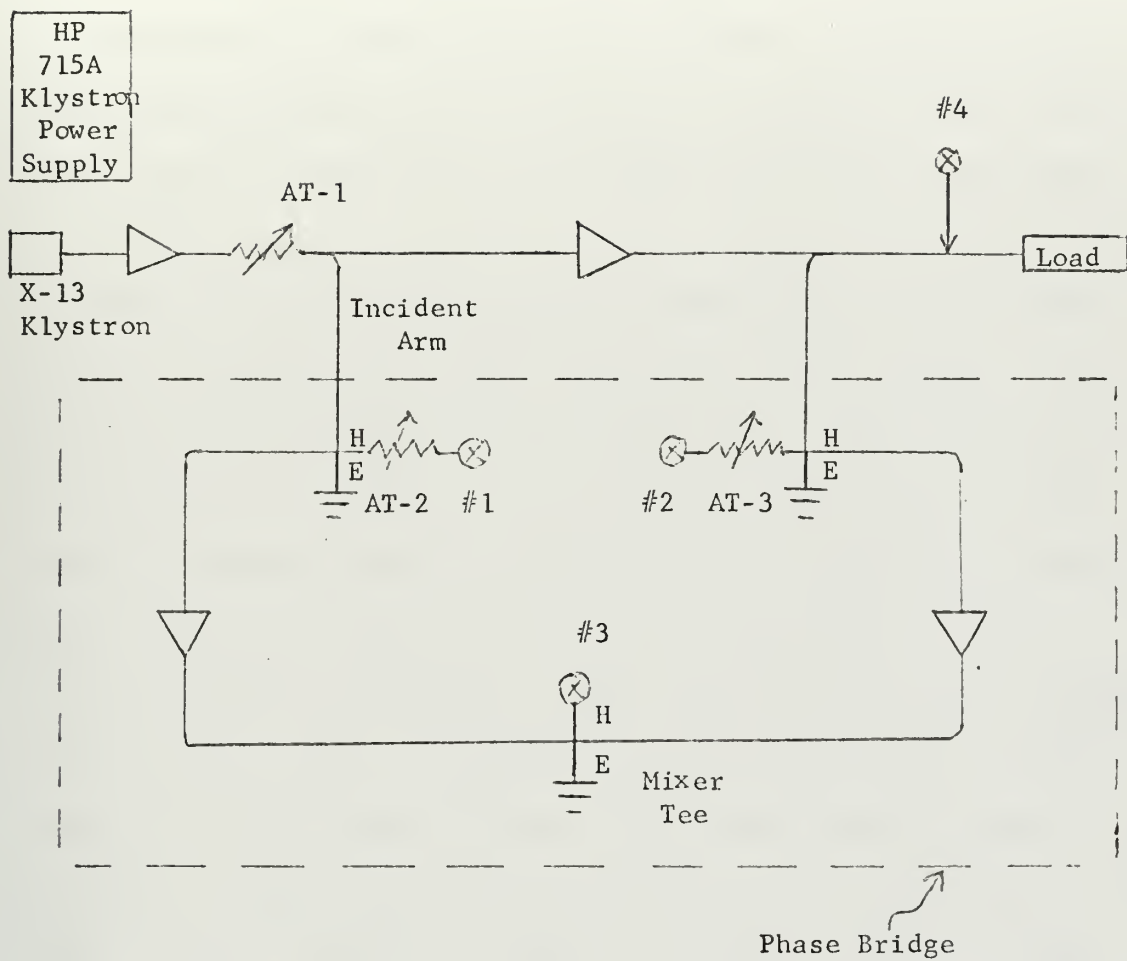


Figure IV-1 Single-Arm System

When the capacitive and inductive loads were connected, the slotted line was removed to reduce any possible losses. A Hewlett Packard Model X910B termination was placed behind the capacitive and inductive loads in order to insure that all reflections were due to the loads themselves.

The directional couplers used for signal inputs to the bridge are Hewlett Packard Model X752C. The signal from the coupler enters the H arm of a Microwave Associates Hybrid Tee. The E arm of the tee is terminated. The signal from one collinear arm of the tee passes through a precision variable attenuator (AT-2) to a Hewlett Packard Model X421A Crystal Detector with a 1N26B crystal (all crystals are labelled Φ on the diagram). This detector measures the amplitude of the incident signal. Attenuator AT-2 was necessary to keep this crystal within its square-law range. The signal from the other collinear arm passes through another Uniline Isolator which was used to prevent interference between the various portions of the bridge. The incident signal then goes to one collinear arm of the hybrid tee used for mixing the incident and reflected signals.

The reflected arm of the system is basically a mirror image of the incident arm. The components of the arm; the crystal detector, isolator, and variable attenuator (AT-3); have analogous functions in the reflected arm. The signal from the reflected arm goes into the other collinear arm of the hybrid tee mixer.

When waves are fed into one collinear arm of a hybrid tee, they do not appear in the other collinear arm because the E arm causes a phase delay and the H arm causes a phase advance. This provides further isolation of the incident and reflected arms of

the incident and reflected arms of the bridge. The H and E arms of the hybrid tee give the sum and difference, respectively, of the waves incident on the collinear arms. Therefore, the hybrid tee combines the waves as a single-ended mixer, as discussed previously in section II.

Although hybrid tees have been used in the above circuit, one will notice that only the H arms and collinear arms have been utilized. The E arm of each hybrid tee has been terminated with a Hewlett Packard Model X910B Termination. Hybrid tees have been used rather than H-plane tees because of the additional isolation they provide. It would be possible to construct this bridge using only E-plane tees or the E arms of the hybrid tees rather than the H arms; however, this gives additional complications in phase determination. There is a phase shift between waves incident on the E arm of a hybrid tee and the output of the collinear arms. Also the outputs of the collinear arms are out of phase with each other with an E arm input. When waves are incident on the H arm of a hybrid tee, no phase change takes place in the output of the collinear arms. Since phase is what this system is designed to determine, any additional phase shifts within the system would only complicate calculations.

Each X421A Crystal Detector and the X444A Crystal Detector are connected directly to Hewlett Packard 415B Standing Wave Indicators. These standing-wave indicators give a direct reading of the crystal output voltage and provide the best load to maximize the crystal's square-law range. Except for the standing-wave indicator connected to the slotted line, the db scale was used on all other indicators and calculations were made based on db.

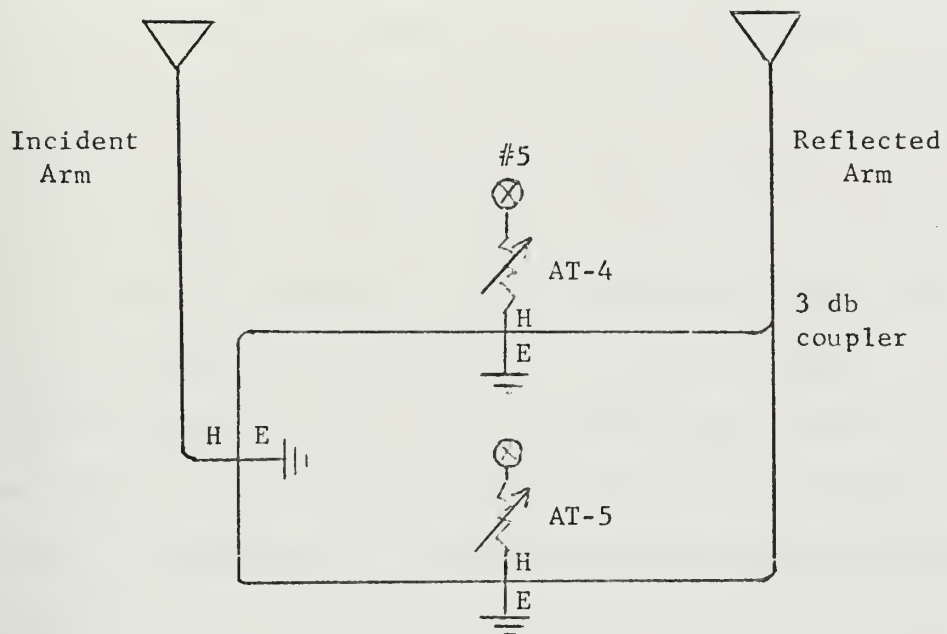


Figure IV-2 Double-Arm System

The phase bridge shown in figure IV-2 utilizes two mixers. All components up to the incident and reflected signal isolators are the same as in the previously discussed system and, therefore, have not been shown again. The incident signal is divided into two in phase components by a hybrid tee. The 3 db directional coupler divides the reflected signal into two equal components, one having its phase shifted 90 degrees. The two components of the incident signal of the reflected signal are added in separate tees which operate as single ended mixers, as described in the previous system. As described in section II, the 90 degree phase shift of one component of the reflected signal means that the output voltage of one mixer is proportional to the cosine of the phase angle between the incident and reflected signals and the other mixer is proportional to the sine of the phase angle. Since two out-put voltages are being measured, there is no need to measure the reflection coefficient separately as in the single arm bridge.

Voltages were measured using Hewlett Packard 415B Standing-Wave Indicators in the same manner as described above.

V. EXPERIMENTAL PROCEDURES AND CALIBRATION

A. PROCEDURES

Once the system was properly calibrated, the experimental procedures were quite simple. The standing-wave indicators were always allowed to warm up a minimum of one hour to insure proper stability. The Klystron power supply was allowed to warm up at least thirty minutes.

With the slotted line in place, a Microwave Associates Waveguide Adjustable Short, Model 546A, was attached as a load. This adjustable short has a range of 0.00 inches to 1.30 inches (3.30 centimeters) or approximately three-quarters of the guide wavelength. With the adjustable short set at 0.00 inches, the guide wavelength was determined by measuring the distance between successive maxima and minima. The voltage standing-wave ratio was also checked to insure that the short had a reflection coefficient of approximately one. Prior to the actual phase measurements, the shift of the minima resulting from the movement of the adjustable short was determined to check for interference effects in the line.

Once the above items were checked, the slotted line was removed from the circuit and the adjustable short was connected directly to the waveguide system. The adjustable short was then moved in 0.050-inch intervals and readings from each of the crystals were recorded. From these readings and the formulae developed in section II, a relationship between phase angle and distance the short was moved (see section VI) was obtained to be used as part of the calibration.

The adjustable short was then replaced by a short constructed from the same material as the inductive and capacitive windows discussed in section III. This short provided the reference phase from which values of inductive and capacitive reactance were determined on the Smith chart. Readings were made for this short and a phase angle computed from the formulae of section II.

Once the reference was obtained, the short was replaced by the inductive and capacitive windows and voltage readings were obtained for each of the seven windows.

Throughout the above procedure, extreme care had to be taken to insure that all of the crystal detectors were kept within their square-law regions. Each detector's square-law region was recorded on the face of its companion standing-wave indicator in order to insure that no measurements were made outside the region. The precision variable attenuators AT-1, AT-2, and AT-3 were adjusted up or down to maintain the square-law response and the settings of these attenuators recorded as part of the data in order to correct the voltage readings.

B. CALIBRATION

One of the major problems encountered during construction of the phase measurement system was calibration. Any time a crystal detector was outside its square-law region, it would give erroneous measurements. Errors in calibration can also result from the differences in calibration of the standing-wave indicators and crystals. Finally, a third item that needed calibration was the losses throughout the system due to the less-than-perfect components, such as

the directional couplers, hybrid tees, isolators, and even losses in the waveguide.

After several false starts and unsuccessful attempts, a procedure for the determination of the square-law region was developed. One of the factors that affected the crystal was adjustment of the standing-wave indicator. It was discovered that any movement of the vernier gain knob shifted the square-law region as much as one decade. Also different combinations of crystal detectors and standing-wave indicators produced slightly different regions. Therefore, in order to obtain a consistent calibration, a crystal detector and standing-wave indicator were calibrated as a set.

The setup used to determine the square-law region for each crystal detector and standing-wave indicator was quite simple [Ref. 2]. It consisted of a precision variable attenuator connected directly to the X-13 Reflex Klystron and then terminated by a crystal detector and standing-wave indicator. The precision variable attenuator was placed at 50 db attenuation and power was applied to the Klystron. The standing-wave indicator was also placed in the 50 db range position by means of the range switch. When the range switch was placed in the 60 db position, noise caused excessive jumping of the needle and measurements were unable to be made with any accuracy. The attenuation was then decreased in increments of 4 db. Both the readings on the precision variable attenuator and the standing-wave indicator were recorded. A plot of two of the crystals used for measurements is shown in fig. V-1. The square-law region is indicated by the solid line.

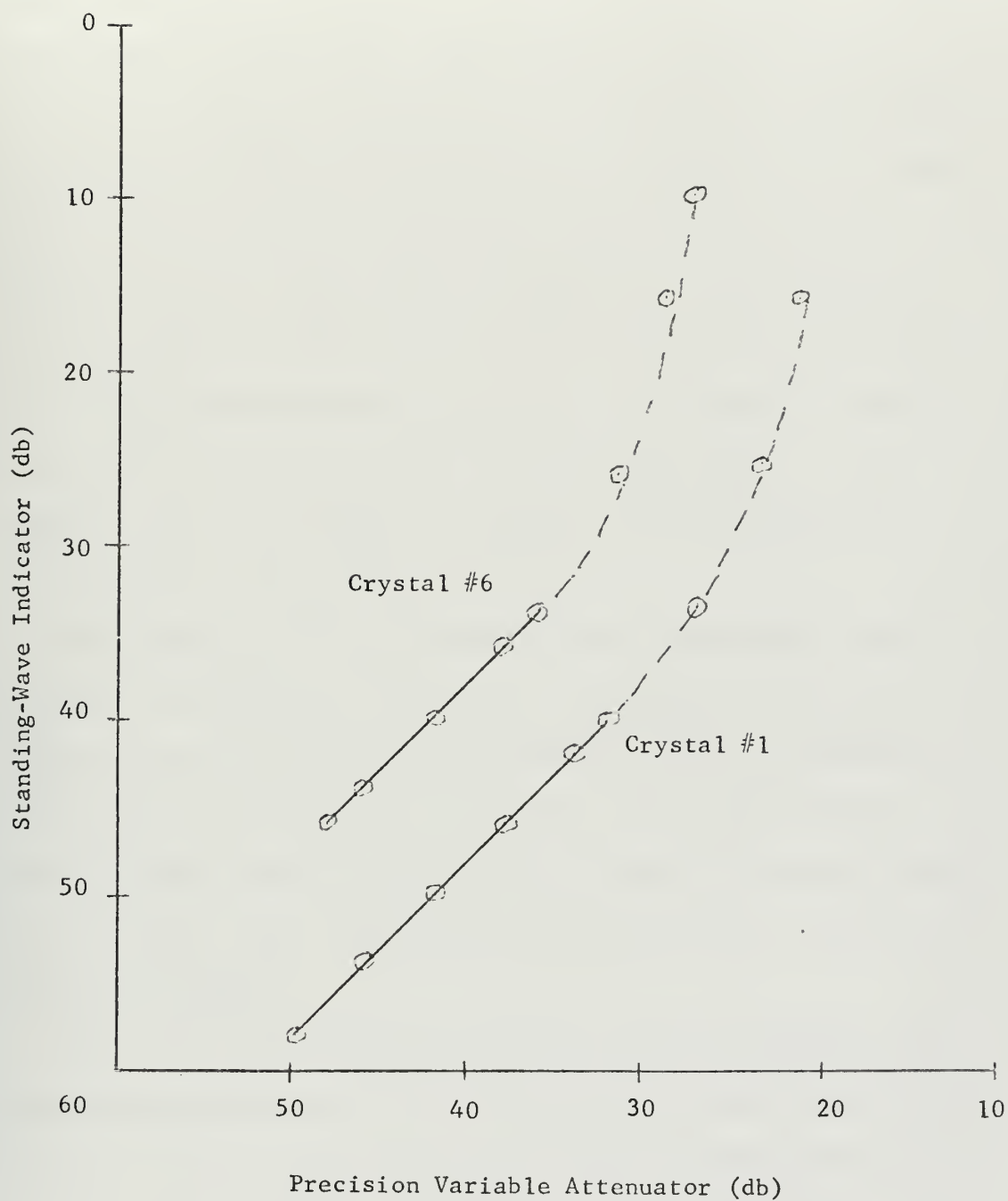


Figure V-1

Figure V-1 is representative of only those crystals with the best characteristics. Several crystals checked had square-law regions of only four or five db. The use of such crystals would have seriously complicated the measurements. It should also be noted that the range of the square-law region varies a large amount from crystal to crystal. For example, crystal number 6 has a range of 46.1 db to 34.1 db, whereas crystal number 1 has a range of 58.0 db to 40.0 db. The method of correcting for the difference in meter readings consisted of measuring each crystal at the location of the incident signal crystal ($\theta = 1$), although any crystal location could have been used. Not all crystals gave the same readings; thus, corrections for different crystal response had to be included as part of the calibration.

The components of the system itself also contributed losses for which corrections had to be made. For example, each of the isolators reduced the power by approximately one db. Additional losses came from the hybrid tees and the directional couplers. Finally, minor losses were created by the length of waveguide needed for the system. Thus, all crystal readings had to be corrected for the various effects.

The meter-crystal pairs at the phase port and reflected port gave readings within 0.1 to 0.2 db of each other when tested, whereas the meter at the incident port gave readings of approximately eleven db above these other two, as determined by this calibration. Since the crystals at the reflected and phase ports were quite similar, it was felt that all corrections could be applied to the measured voltage at the incident port.

A relationship among the incident, reflected, and phase voltages was determined from equation II-7. Experimentally, the phase angle was shifted 180 degrees by moving the adjustable short $\lambda/4$ and values for the incident, reflected, and phase voltages were determined. These experimental values were compared (using equation II-7) and it was found that a correction of 11.7 db to the incident voltage was necessary. Eleven db was known to be due to the meter differences; therefore, the other 0.7 was assumed to be line loss. This 11.7 db correction was applied to all subsequent incident voltage readings.

IV. RESULTS

The use of the slotted line verified that the maximum was a distance of $\lambda_g/4$ from the first minimum and that the two minima were $\lambda_g/2$ apart. The graph in fig. VI-1 is a plot of the phase crystal voltage in db versus the phase shift in wavelength for a single-arm bridge. As expected, the minima occur at phase shift intervals of zero and 2π and the maximum occurs at π . This confirmed that use of equation II-7 is proper for the calculation of relative phase angles from measured voltages for this system.

A similar graph (fig. VI-2) is shown for the double-arm system. As can be seen, the minima are quite undefined and the maxima quite flattened out as compared with the single-arm system. There are two possible explanations for the undefined minima. One is that the source is not putting out a completely pure signal and that mixed modes are present. The other possibility is that, because of the additional waveguide components, there are internal reflections in the system.

Tables VI-1 and VI-2 are a compilation of the results for the single-arm phase measurement system. Seven irises were used as sample loads, four were inductive (I-1 through I-4) and three were capacitive (C-1 through C-3). In Table VI-1, we show the dimension of the irises. $(B/Y_o)_{\text{theoretical}}$ gives the relative susceptances calculated from equations III-3 and III-4. $\phi_{\text{theoretical}}$ is the phase angle determined from the Smith chart using the calculated susceptances and assuming that the iris is purely imaginary. In Table VI-2, the

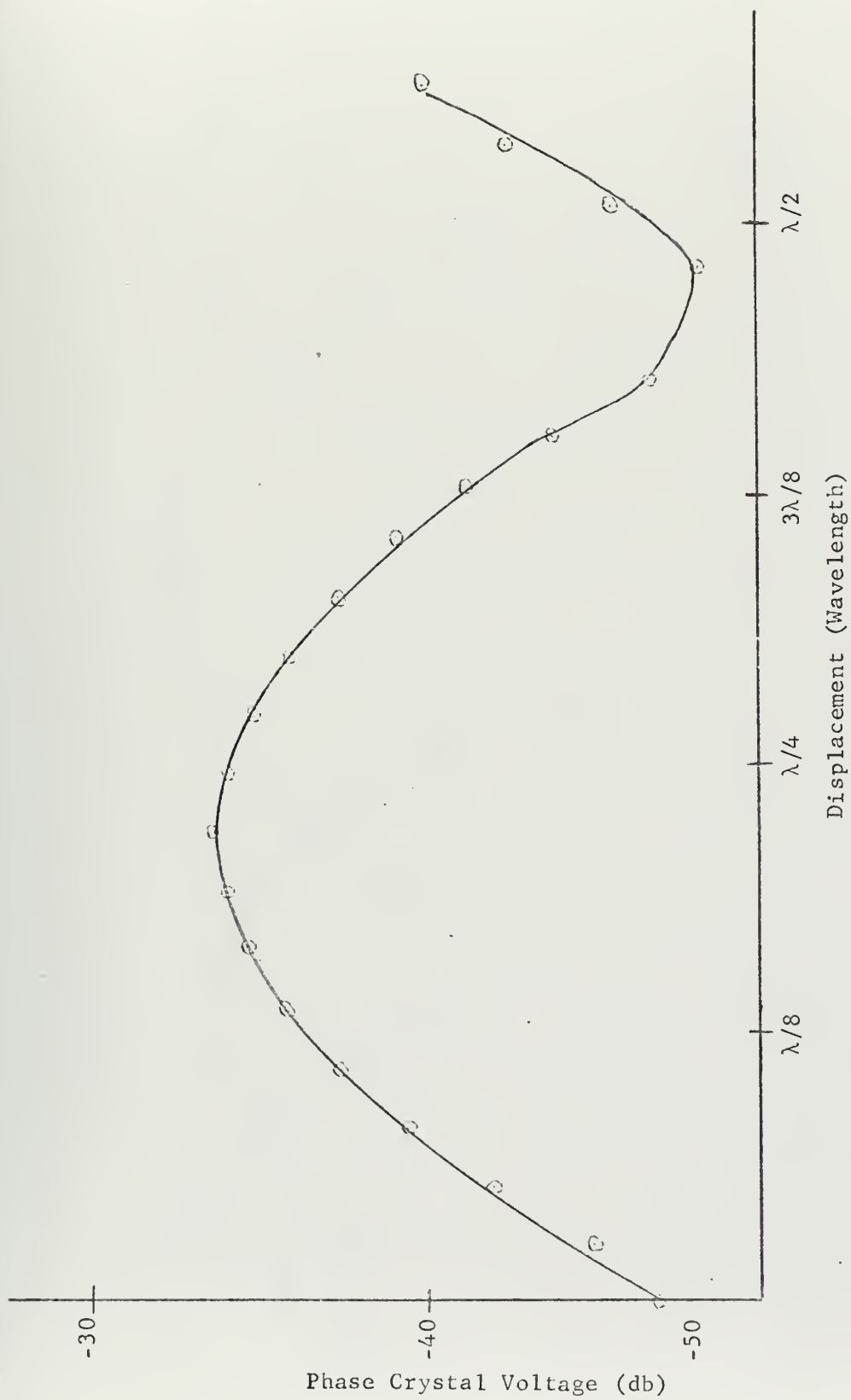


Figure VI-1 Plot of Phase Crystal Voltage vs Displacement for Single-arm System

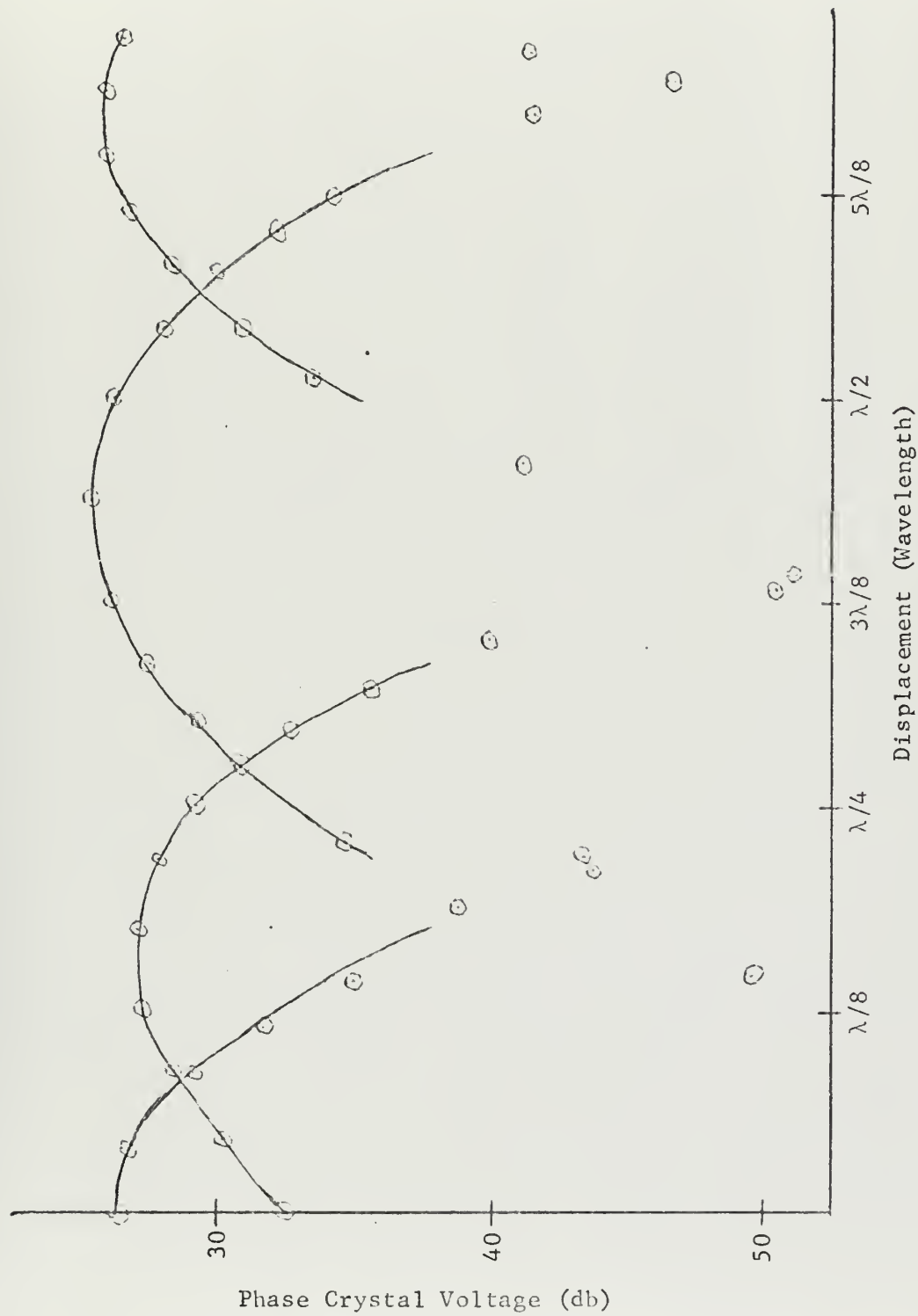


Figure VI-2 Plot of Phase Crystal Voltage vs Displacement for Double-arm System

Iris	$(B/Y_o)_{cal}$	ϕ_{theo}	ϕ_{corr}
I#1	3.417	31°	30°
I#2	2.047	44°	45°
I#3	1.424	54°	53°
I#4	1.003	63°	56°
C#1	0.701	71°	80°
C#2	0.500	76°	90°
C#3	0.367	80°	104°

Table VI-1

Iris	r	V	ϕ_{meas}	$\frac{B}{Y_0}_{\text{meas}}$	$\Delta\phi$
I#1	.891	27.6	27°	3.95	3°
I#2	.760	28.7	41°	2.30	4°
I#3	.631	28.7	49°	1.68	4°
I#4	.514	28.2	54°	1.28	2°
C#1	.485	23.2	68°	1.02	12°
C#2	.372	23.5	80°	0.72	10°
C#3	.282	23.8	96°	0.49	8°

Table VI-2

reflection coefficient, r , was taken as the ratio of the corrected readings for the incident and reflected signals. V is the corrected reading at the phase port. ϕ_{measured} was determined from equation II-7 using the corrected V and r . ϕ_{measured} and r gave a point on the Smith chart from which the measured conductance and susceptance are determined. $(B/Y_o)_{\text{measured}}$ is listed in Table VI-2. The theoretical and measured susceptances can be compared between the two tables.

If the irises were purely imaginary, the measured conductance should be 1.0. These values ranged from 0.85 to 1.15 leading to the error between $(B/Y_o)_{\text{theoretical}}$ and $(B/Y_o)_{\text{measured}}$. Correction for this effect was made as follows. The measured conductance and the calculated susceptance were used to plot a new point on the Smith chart, and a new phase angle, $\phi_{\text{corrected}}$ indicated in Table VI-1, was determined. This is the angle we compare with ϕ_{measured} . It is felt that this is the best method to use to correct for the real portion of the iris admittance. The last column in Table VI-2 gives the difference between the measured phase angle and the corrected theoretical phase angle, $\Delta\phi$.

As can be seen from Table VI-2, the results for the inductive irises are accurate to about four degrees, whereas the capacitive irises are only accurate to approximately ten degrees. A possible explanation for this is that the phase angles for the capacitive irises are close to 90 degrees. Throughout the experiment, it was found that computations for angles near 90 degrees were extremely sensitive to errors because of the rapid change of the cosine with only slight differences in the measured parameters near that angle.

VII. CONCLUSIONS

Several things contributed errors to the results. The largest source of error was created by the system components. As discussed previously, much time had to be devoted to calibrating crystals, and unmatched crystals probably contributed the greatest source of error. A check of the hybrid tees and couplers also revealed that they did not split the power perfectly as required. It was also noted during the early stages of experimentation that curved sections of waveguide caused variations in the measurements. Finally, additional errors were present because of the mismatch created when the waveguide components were joined.

Other errors were caused by possible mixed modes from the source, temperature variations affecting the crystals, and internal reflections caused by the system itself.

The results obtained from the single-arm system were fairly accurate for the inductive irises; however, the results for the capacitive irises can only be considered fair. Also the recording of measurements was slow since readings from each attenuator had to be recorded. Since the objective was to design an accurate, rapid measurement system, this system was not accurate or fast enough. Therefore, the construction of an accurate phase measurement system with components available in the laboratory is not considered feasible. It is possible, however, that a more accurate system could be designed if well-matched components were used. This would create additional expense, however, which might not be justifiable.

If the construction of a phase bridge system is still necessary, it is recommended that the incident and reflected arms be equal in length. Because of the necessity that the phase measurement system cover a wide frequency range, equal lengths in these arms will prevent phase shifts due to changes in frequency. In addition, it is recommended that the use of balanced mixers be explored more fully and, if successful, that they be applied to the full phase bridge discussed by Dyson.

LIST OF REFERENCES

1. Dyson, J. D., "The Measurement of Phase of UHF and Microwave Frequencies," IEEE Transactions on Microwave Theory and Techniques, v. Mtt-14, p. 410-423, September 1966.
2. Ginzton, E. L., Microwave Measurements, McGraw-Hill, 1957.
3. Montgomery, C. G., Dicke, R. H., and Purcell, E. M., Principles of Microwave Circuits, McGraw-Hill, 1948.
4. Hewlett-Packard Company, Microwave Theory and Measurements, Prentice-Hall, 1962.
5. Montgomery, C. G., Techniques of Microwave Measurements, McGraw-Hill, 1947.
6. Ishii, T. K., Microwave Engineering, Ronald Press Company, 1966.

INITIAL DISTRIBUTION LIST

	No. Copies
1. Defense Documentation Center Cameron Station Alexandria, Virginia 22314	2
2. Library, Code 0212 Naval Postgraduate School Monterey, California 93940	2
3. Prof. G. E. Schacher, Code 61Sq Department of Physics Naval Postgraduate School Monterey, California 93940	1
4. Major William A. Weis 5 Church St. East Bloomfield, New York 14443	1

DOCUMENT CONTROL DATA - R & D

(Security classification of title, body of abstract and indexing annotation must be entered when the overall report is classified)

1. ORIGINATING ACTIVITY (Corporate author) Naval Postgraduate School Monterey, California 93940		2a. REPORT SECURITY CLASSIFICATION Unclassified	
		2b. GROUP	
3. REPORT TITLE The Design and Evaluation of a Microwave Phase Measurement System			
4. DESCRIPTIVE NOTES (Type of report and, inclusive dates) Master's Thesis; June 1971			
5. AUTHOR(S) (First name, middle initial, last name) William A. Weis			
6. REPORT DATE June 1971	7a. TOTAL NO. OF PAGES 42	7b. NO. OF REFS 6	
8a. CONTRACT OR GRANT NO.		9a. ORIGINATOR'S REPORT NUMBER(S)	
b. PROJECT NO.			
c.		9b. OTHER REPORT NO(S) (Any other numbers that may be assigned this report)	
d.			
10. DISTRIBUTION STATEMENT Approved for public release; distribution unlimited.			
11. SUPPLEMENTARY NOTES		12. SPONSORING MILITARY ACTIVITY Naval Postgraduate School Monterey, California 93940	
13. ABSTRACT <p>This thesis was undertaken to ascertain the feasibility of producing an accurate phase measurement system using standard components normally available in the laboratory or those that could be purchased relatively inexpensively. Several systems are discussed and two of them were physically evaluated. It was concluded that it was not feasible to build an accurate system without large additional expense; however, if such expense is justifiable, recommendations are given for the construction of an improved system.</p>			

KEY WORDS	LINK A		LINK B		LINK C	
	ROLE	WT	ROLE	WT	ROLE	WT
Phase Measurement						
Susceptance						
Microwave System						
Transmission Lines						
Waveguides						

Thesis
W375
c.1

Weis

128219

The design and eval-
uation of a microwave
phase measurement sys-
tem.

Thesis
W375
c.1

Weis

128219

The design and eval-
uation of a microwave
phase measurement sys-
tem.

thesW375

The design and evaluation of a microwave



3 2768 001 95181 7

DUDLEY KNOX LIBRARY